Communication

A Homochiral Nanotubular Crystalline Framework of Metallomacrocycles for Enantioselective Recognition and Separation

Gao Li, Weibin Yu, and Yong Cui

J. Am. Chem. Soc., **2008**, 130 (14), 4582-4583 • DOI: 10.1021/ja078317n

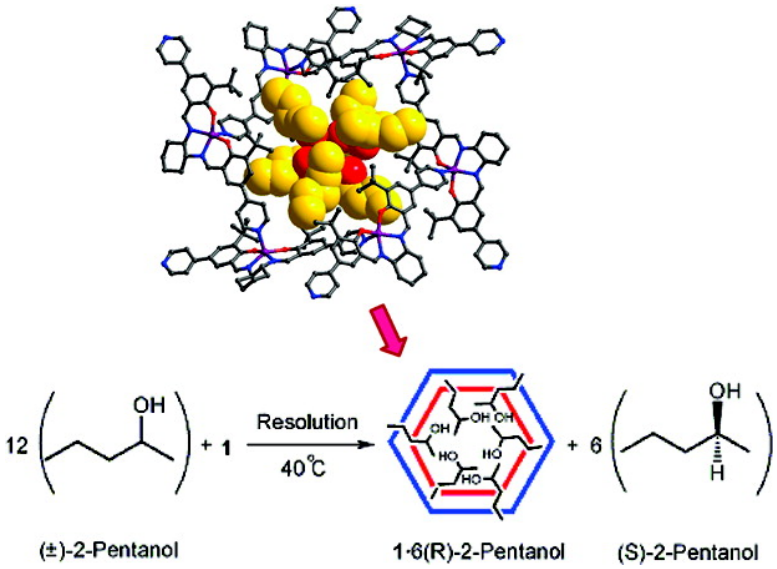

More About This Article

Additional resources and features associated with this article are available within the HTML version:

- Supporting Information
- Links to the 1 articles that cite this article, as of the time of this article download
- Access to high resolution figures
- Links to articles and content related to this article
- Copyright permission to reproduce figures and/or text from this article

View the Full Text HTML

J|A|C|S
COMMUNICATIONS

Published on Web 03/18/2008

A Homochiral Nanotubular Crystalline Framework of Metallomacrocycles for Enantioselective Recognition and Separation

Gao Li, Weibin Yu, and Yong Cui*

School of Chemistry and Chemical Technology, Shanghai Jiao Tong University, Shanghai 200240, China

Received October 31, 2007; E-mail: yongcui@sjtu.edu.cn

Nanotubular architectures, and in particular carbon nanotubes, have received considerable attention due to their potential applications in nanoelectronics, molecular devices and sensors, ion exchange, and catalysis.[1] Although single-walled carbon nanotubes can exist in chiral forms,[2] recent theoretical studies indicated that their chiral species cannot be used as enantiospecific adsorbents due to the lack of functional groups.[3] The supramolecular self-assembly of intrinsically chiral organic and metallaorganic building blocks, on the other hand, provides especially intriguing opportunities to make well-defined nanotubular architectures.[4] The ability to incorporate other functionalities into such assembled entities will expand their utility in enantioselective processes. However, only a few examples of chiral nanotubular assemblies have been reported to date, and their applications in enantioselective processes have not yet been explored.[5−7] Rigid and shape-persistent organic macrocycles are versatile building blocks for supramolecular design and ideally suited for the hierarchical assembly into nanotubes with utilizable functional groups;[8] self-assembly of hollow tubular structures from cyclic peptides and cyclodextrins based on noncovalent interactions are exemplary cases.[7]

We report here the assembly of a homochiral nanotubular crystalline material from nanoscale $Zn_6\mathbf{L}_6$ metallacycles featuring self-complementary metallosalen ZnL motifs ($H_2\mathbf{L}$ = (*R*,*R*)-(−)-*N*,*N*′-bis(3-*tert*-butyl-5-(4-pyridyl) salicylidene)-1,2-diamino-cyclohexane) by using THF as templates[6c,9] and demonstrate its ability to undergo highly enantioselective recognition and separation. Single crystals of $[Zn_6\mathbf{L}_6]\cdot 6THF$ (**1**·6THF) were obtained in good yield by heating a mixture of $Zn(NO_3)_2\cdot 6H_2O$ and ($H_2\mathbf{L}$) (1:1 molar ratio) in DMF, THF, and water at 80 °C for 1 day. The product is stable in air and insoluble in water and common organic solvents and was formulated on the basis of microanalysis, IR, and thermogravimetric analysis (TGA).

1·6THF crystallizes in the trigonal chiral space group *R*3, with one-third of a molecule in the asymmetric unit, and exhibits a tubular architecture.[10] The Zn centers adopt a square pyramidal geometry with the equatorial plane occupied by the central N_2O_2 donors of one **L** ligand and the apical position by one pyridine of another **L** ligand. Each Zn**L** unit thus uses one terminal pyridyl group to coordinate a Zn atom building a hexamer and remains with one pyridine uncoordinated. The cyclic hexamer has an outer diameter of 4.01 nm, a height of 1.19 nm, and an inner pore diameter of 1.20 nm. The distances between adjacent zinc atoms are 11.5834(5) and 11.5802(3) Å, and the distance between opposite zinc atoms is 21.9256(6) Å. The two independent zinc centers are both 0.42 Å above the plane formed by N_2O_2 coordination sites toward the axial pyridyl group. The equatorial ZnN_2O_2 planes make dihedral angles of 22.39° and 25.65° with the coordinated pyridine rings and of 28.47° and 28.51° with the uncoordinated pyridine rings. The six pairs of *tert*-butyl groups of **L** ligands are organized in a manner that partly cover two sides of the cyclic hexamer along its crystallographic threefold axis, thus generating six hydrophobic pockets, each of which is occupied by one THF molecule. The guest templating effect in **1** is inferred from the presence of weak hydrophobic interactions between the ligand methyl groups and solvent methyl groups (Figure S1).

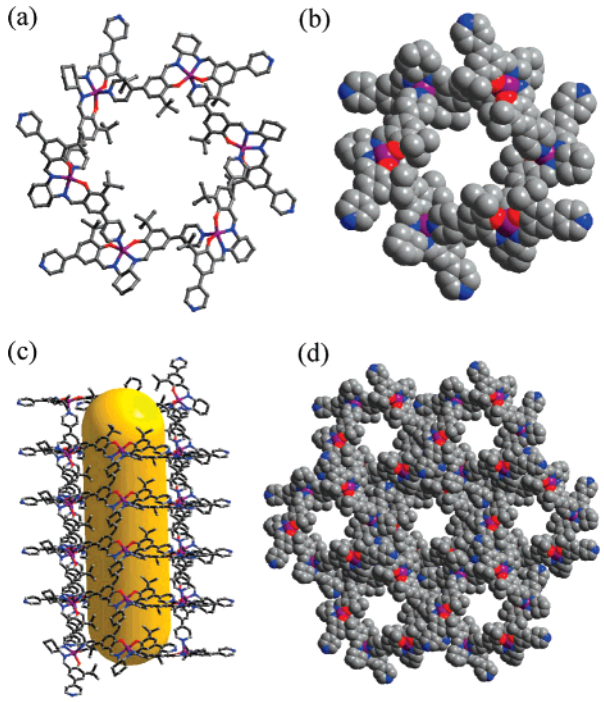

Figure 1. (a) A view of the molecular structure of Zn_6L_6 in **1** and (b) its space-filling mode. (c) Packing of Zn_6L_6 macrocycles to generate a nanotube. (d) A space-filling mode showing the open channels along the *c*-axis within the 3D supramolecular structure of **1**. The included guest molecules were omitted for clarity.

Strong CH···π interactions between the butyl group and the conjugated pyridine ring of adjacent metallacycles (C−H···π = 2.96 −3.25 Å) direct packing of metallacycles in parallel along the crystallographic *c*-axis, making a nanosized tubule with an interrupted channel (opening size: 1.4 nm × 1.1 nm). The structure is reinforced by face-to-face intermolecular $\pi-\pi$ interactions; each Zn_6L_6 unit is engaged in six sets of such $\pi-\pi$ stackings (plane-to-plane separation = 3.27 Å) through its extended π conjugated parts. Additional CH···π (2.95−3.05 Å) and CH···N (3.00−3.15 Å) interactions between uncoordinated pyridyl groups and aromatic rings of ZnL units further strengthen the nanotubes (Figures S3−S7). Highly directional noncovalent interactions in **1** thus have clearly steered the packing of macrocyles into a homochiral porous 3D nanotubular architecture (Figure 1d).

Calculations using PLATON indicate that **1** has 24.0% of the total volume occupied by solvent molecules.[11] TGA revealed that the six THF guest molecules could be removed in the temperature range from 80 to 130 °C. Powder XRD experiments indicate that

10.1021/ja078317n CCC: $40.75

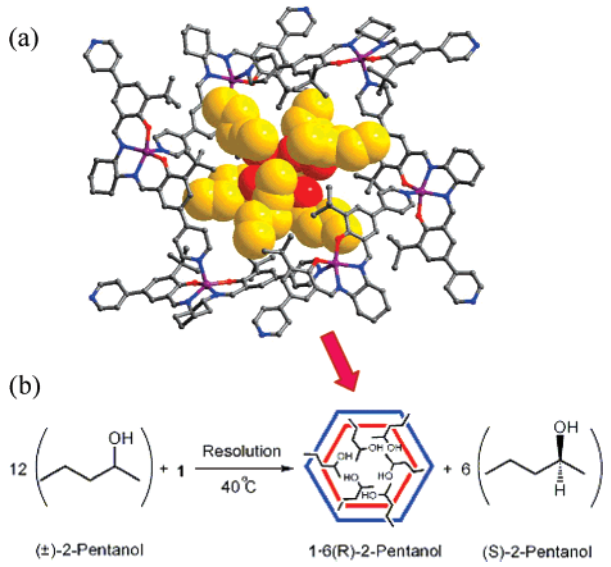

Figure 2. (a) A view showing the inclusion of six (*R*)-2-pentanol molecules (drawn in space-filling style) in **1**. (b) A view showing selective inclusion of (*R*)-2-pentanol into nanotubular channels of **1**.

the framework and crystallinity of **1** remain intact upon complete removal of guest molecules. The permanent porosity of **1** was confirmed by its N_2 adsorption isotherm at 77 K. After desolvation, **1** exhibits a Type-I sorption behavior, with a Langmuir surface area of 504 m^2/g and a pore volume of 0.48 mL/g (Figure S11).

To investigate whether **1** allows enantioselective separation, its evacuated single-crystals were soaked in neat racemic 2-pentanol in a sealed vial at 40 °C. After 2 days, most crystals remained transparent but with apparent fracturing. This inclusion of 2-pentanol is supported by microanalysis, TGA, and powder XRD (Figures S8 and S10). Single crystals suitable X-ray diffraction were obtained by heating **1**·6THF in 2-pentanol for 3 days. The solid-state structure clearly revealed that the **1**·6(*R*)-2-pentanol adduct is isostructural to **1**·6THF and (*R*)-2-pentanol has been included in the chiral channel of **1** (Figure 2).[9] The cell volume of adduct **1** increases by 2.6% as THF molecules were replaced by pentanol molecules in the structure. Although the tubular skeleton is intact, the Zn**L** units undergo rotational rearrangements upon including larger guest molecules. In particularly, the equatorial ZnN_2O_2 planes make dihedral angles of 27.48° and 29.47° with the coordinated pyridine ring and of 32.70° and 32.98° with the uncoordinated pyridine rings, all of which are obviously larger than those in **1**·6THF and are caused by the axis rotation of pyridine rings. Six free alcohol molecules are trapped in six pockets of the macrocycle and form weak hydrophobic interactions through their methyl groups. More interestingly, the hydroxy groups of six alcohol molecules form strong hydrogen bonds (O···O = 2.711 and 2.927 Å) leading to a chair-shaped conformation.

Chiral GC analysis of the 2-pentanol desorbed from **1** showed that the enantiomeric excess (ee) value was 99.5%, whereas the absolute configuration of (*R*)-2-pentanol was confirmed by comparison of the retention time with that of the reported example. Similar enantioselective inclusion behaviors are observed for racemic 2-butanol and 3-methyl-2-butanol, whereby **1** exhibited remarkable sorption toward the *R* enantiomer over the *S* enantiomer as well (Figures S12 and S13).[12] The inclusion compounds can be respectively formulated as **1**·6(2-butanol) and **1**·6(3-methyl-2-butanol) based on microanalysis, TGA, and powder XRD. The ee values of desorbed (*R*)-2-butanol and (*R*)-3-methyl-2-butanol were 98.4% and 95.6%, respectively.

We have also successfully recycled and reused **1** for resolving racemic alcohol without the deterioration of enantioselectivity. **1** was used for five cycles of separation of racemic 2-butanol without loss of enantioselectivity (98.4, 98.2, 98.3, 98.0, and 97.8% ee for 1−5 runs, respectively). Moreover, the crystallinity of **1** was well retained even after 5 runs (Figures S9 and S13). However, attempts to separate racemic 2-hexanol by using **1** have thus far been unsuccessful. Further investigations on the resolution of other racemic molecules are currently underway.

In conclusion, we reported the efficient assembly of a nanotubular supramolecular structure based on hexametallic macrocycles. Chiral channel and hydrophobic functionality presented by **1** make it an excellent host to recognize and separate racemic alcohols with high enantioselectivity (up to 99.5%). The ready tunability of such a molecular building-block approach promises to lead to unique and practically useful chiral sorbents.

Acknowledgment. This work was supported by NSFC-20671062, "973" Program (2007CB209701), NCET-05-0395, Key Project of Basic Research of Shanghai (05JC14020), and Shuguang Program (06SG12).

Supporting Information Available: Details of experiments, structure, XRD patterns, TGA, GC, and full X-ray crystallographic information in CIF format. This material is available free of charge via the Internet at http://pubs.acs.org.

References

(1) (a) Fenniri, H.; Mathivanan, P.; Vidale, K. L.; Sherman, D. M.; Hallenga, K.; Wood, K. V.; Stowell, J. G. *J. Am. Chem. Soc.* **2001**, *123*, 3854. (b) Ranganathan, D.; Lakshmi, C.; Karle, I. L. *J. Am. Chem. Soc.* **1999**, *121*, 6103. (c) Dai, H. *Acc. Chem. Res.* **2002**, *35*, 998.
(2) Mintmire, J. W.; White, C. T. *Phys. Rev. Lett.* **1998**, *81*, 2506.
(3) Power, T. D.; Skoulidas, A. I.; Sholl, D. S. *J. Am. Chem. Soc.* **2002**, *124*, 1858.
(4) (a) Holliday, B. J.; Mirkin, C. A. *Angew. Chem., Int. Ed.* **2001**, *40*, 2022. (b) Leininger, S.; Olenyuk, B.; Stang, P. J. *Chem. Rev.* **2000**, *100*, 853. (c) Conn, M. M.; Rebek, J., Jr. *Chem. Rev.* **1997**, *97*, 1647.
(5) (a) Cui, Y.; Lee, S. J.; Lin, W. *J. Am. Chem. Soc.* **2003**, *125*, 6014. (b) Orr, G. W.; Barbour, L. J.; Atwood, J. L. *Science* **1999**, *285*, 1409. (c) Pantos, G. D.; Pengo, P.; Sanders, J. K. M. *Angew. Chem., Int. Ed.* **2007**, *46*, 194.
(6) (a) Xiong, R.-G.; You, X.-Z.; Abrahams, B. F.; Xue, Z.; Zhe, C.-M. *Angew. Chem., Int. Ed.* **2001**, *40*, 4422. (b) Song, Y.-M.; Zhou, T.; Wang, X.-S.; Li, X.-N.; Xiong, R.-G. *Cryst. Growth Des.* **2006**, *6*, 14. (c) Li, G.; Yu, W.; Ni, J.; Liu, T.; Liu, Y.; Sheng, E.; Cui, Y. *Angew. Chem., Int. Ed.* **2008**, *47*, 1245.
(7) Bong, D. T.; Clark, T. D.; Granja, J. T.; Ghadiri, M. R. *Angew. Chem., Int. Ed.* **2001**, *40*, 988.
(8) (a) Moore, J. S. *Acc. Chem. Res.* **1997**, *30*, 402. (b) Leininger, S.; Olenyuk, B.; Stang, P. J. *Chem. Rev.* **2000**, 100, 853. (c) Shimizu, L. S.; Hughes, A. D.; Smith, M. D.; Davis, M. J.; Zhang, B. P.; Zur Loye, H. C.; Shimizu, K. D. *J. Am. Chem. Soc.* **2003**, *125*, 14972. (d) Gallant, A. J.; MacLachlan, M. J. *Angew. Chem., Int. Ed.* **2003**, *42*, 5307.
(9) Sun, S.-S.; Stern, C. L.; Nguyen, S. T.; Hupp, J. T. *J. Am. Chem. Soc.* **2004**, *126*, 6314.
(10) Crystal data for **1**·6THF: trigonal, *R*3, a = 44.861(6) Å, c = 10.203(2) Å, V = 17783(5) Å^3, D_{calcd} = 1.217 g/cm^3, Z = 3, R_1 = 0.0423 ($I > 2.0\sigma(I)$), wR_2 = 0.1182, GOF = 1.065, Flack parameter = 0.04(1). Crystal data for **1**·6Pentanol: trigonal, *R*3, a = 45.0370(19) Å, c = 10.3862(9) Å, V = 18244.3(19) Å^3, D_{calcd} = 1.213 g/cm^3, Z = 3, R_1 = 0.0646, ($I > 2.0\sigma(I)$), wR_2 = 0.1462, GOF = 1.001, Flack parameter = 0.06(2).
(11) Spek, A. L. *PLATON*, version 1.62; University of Utrecht: 1999.
(12) (*S*)-**1** exhibits excellent selectivity for inclusion of the *S* enantiomer over the *R* enantiomer (Figures S14 and S15).

JA078317N